Optical and Quantum Electronics (2022) 54:288
https://doi.org/10.1007/s11082-022-03676-x

Efficient way for chemicals identification using hexagonal fiber with the terahertz (THz) band

Md. Selim Hossain[1] · M. M. Kamruzzaman[2] · Md. Mizanur Rahman[3] · Shuvo Sen[4] · Mir Mohammad Azad[5]

Received: 31 August 2021 / Accepted: 12 March 2022 / Published online: 11 April 2022

Abstract

To detect chemicals, we proposed a photonic crystal fiber (PCF) with hexagonal cladding and a hexahedron core (THz). Circular air holes (CAHs) in the vestibule provide the basis of the suggested sensor. To develop and evaluate our suggested hexahedron PCF sensor, we employed the finite element (FEM) technique and perfectly matched layers (PML), which utilized the optical parameters numerically. Here, 92.65%, 95.25%, and 90.70% are relatively sensitive, and confining losses are low. The value 5.40×10^{-08}, 6.70×10^{-08} dB/m, and 5.75×10^{-08} dB/m for three chemicals such as Ethanol (n = 1.354), Benzene (n = 1.366) and Water (n = 1.330) and effective material loss (EML) of 0.00694 cm^{-1}. The suggested Hx-PCF sensor has been successfully tested at 1 THz. We are certain that the suggested sensor's optimal geometric structure can be manufactured and that it can contribute to real-world applications in biomedicine and industry. In terahertz areas, our suggested PCF fiber is also suited for a wide range of medical signals and applications (THz).

This article is part of the Topical Collection on Optical and Quantum Sciences in Africa.

Guest edited by Salah Obayya, Alex Quandt, Andrew Forbes, Malik Maaza, Abdelmajid Belafhal and Mohamed Farhat.

✉ Shuvo Sen
shuvombstu.it12009@gmail.com

Md. Selim Hossain
selimtee@gmail.com

[1] Department of Computing and Information System (CIS), Daffodil International University, Dhaka, Bangladesh

[2] Department of Computer Science, College of Computer and Information Sciences, Jouf University, Sakakah, Kingdom of Saudi Arabia

[3] Department of Electrical and Electronic Engineering, Hajee Mohammad Danesh Science and Technology University, Dinajpur 5200, Bangladesh

[4] Department of Information and Communication Technology (ICT), Mawlana Bhashani Science and Technology University (MBSTU), Santosh, Tangail 1902, Bangladesh

[5] Department of Computer Science and Engineering, Hamdard University Bangladesh, Dhaka, Bangladesh

Keywords Hexagonal cladding PCF · Hexahedron core · EML · PCF · Scattering loss · Etc

1 Introduction

Finding a chemicals anyplace on the planet is a needed effort, and detecting an unknown substance is a fascinating issue in research. Researchers are creating and designing new types of sensors to fulfill society's demands. Some of these substances are toxic to humans. Because it is considered the major ingredient, ethanol is a sort of chemical that is extensively used for a variety of reasons (Mou et al. 2020a). The alcohol and water components provide the majority of chemical solutions, and these two are regarded as the primary analyzers (Vera et al. 2018). Because alcohol is colorless and has no flow, there has been a lot of study into how to detect it (types of chemical sensing Ho et al. 2008; Rana et al. 2018a). For the safety of our health, an easy and accurate chemical sensing technique is therefore required. Photonic crystal fiber (PCF) has some distinct advantages over traditional fiber and is a boon to modern fiber-optic communication. This boosts communications sectors like telephony, various sensing types, and so forth (Hossain et al. 2021c; Zhou and Zheng 2019). Total internal reflection is the primary method for propagating light throughout a PCF with minimum confinement loss (Hossain et al. 2021b), high nonlinearity (Mollah et al. 2021; Ilatikhameneh et al. 2018; Chen et al. 2006), zero-dispersion (Lu et al. 2008), and other properties. Such unique characteristics (guiding light) have propelled the PCFs to the forefront of liquid and dangerous chemical sensing. In addition to certain optical properties, namely effective material loss (EML) (Ritari et al. 2004), birefringence (Hossain et al. 2021b), dispersion, confinement loss (Abdullah-Al-Shafi et al. 2021; Lee et al. 2002) or absorption loss (Hasan et al. 2021), etc., this also causes a detection barrier. For several types of PCF architecture, the qualities listed above are examined in Shuvo et al. (2020), Hossain et al. (2021c). In Islam et al. (2018a), Hossain et al. (2021d), Ahmen et al. (2017) some outstanding works on chemical sensing were reported. Various types of PCF sensors for different types of analysis are mentioned in Hasanuzzaman et al. (2015), Rahman et al. (2019), Gangwar and Singh (2016), Hasan et al. (2017), Lee et al. (2016), Hossain et al. (2021e). THz waves (from 0.1 to 10 THz) create a new era in the research field of fiber optic communication (Islam et al. 2015a), biomedical engineering (Hasan et al. 2016a), chemical sensing (Islam et al. 2016a), etc. This region covers the gap between microwave and infrared rays. THz sensing is more practicable than other sensors because of its great spatial resolution and lack of ionizing effects.

Recently, several research projects in the THz region related to chemical sensing have been conducted. Hasanuzzaman et al. (2015) have recently achieved a 65.18% sensitivity through a folded PCF-shaped cladding. In 2017, alcohol sensitivity was also achieved with a porous PCF structure (Rana et al. 2018b) of 69.09%. Using the TOPAS as a background material respectively for Benzene, Ethanol, and Water (Sultana et al. 2018). The authors reported that the fluids (tabuns and sarin liquids) were 64% sensitive in Mou et al. (2019) using hexahedron cored PCF. Polytetrafluorethylene was used in (Mou et al. 2019) as background material and a slow core PCF to achieve 77.08%, 77.18%, and 77.23% sensitivity for Benzene, Ethanol, and Water, respectively. Because all of the studies mentioned above do not reveal a suitable level of Sensitivity, there are opportunities to improve Sensitivity.

We introduced the hexahedron PCF in this study to increase relative sensitiveness in the recognition of biochemicals and to reduce production simplification by making the geometric structure of the PCF simple. We have altered the core size and distance between

the air holes to discover the ideal structural conditions, with low containment loss and low effective material loss. As a result, the proposed Hexahedron PCF sensor has an effective wide area, enabling the insertion of a high volume of the analyte. Furthermore, our proposed H_X-PCF has the maximum relative Sensitivity after comparing the previous articles published (Hasan et al. 2016b, c; Ahmed et al. 2017; Rana et al. 2014; Saiful Islam et al. 2018a, b; Hasanuzzaman et al. 2016) that are 92.65%, 95.25%, and 90.70%, and low CLs with the value of 5.40×10^{-08}, 6.70×10^{-08} dB/m, and 5.75×10^{-08} dB/m for three chemicals such as Ethanol, Benzene, and Water where EML is 0.00694 cm^{-1} at monitoring conditions of 1 THz for the detection chemicals in the terahertz regime.

2 Design methodology

A hexagonal cladding, a hexahedron's core area, and field mode supplies for polarization of x and y at 1 THz are shown in Fig. 1, which shows the Hx-geometry. PCF's there are A_1 and d1 for the cladding surface, and Ac and dc for the core surface of the hexahedron. The first layer of six circular air holes is located in the hexahedron's core area. TOPAS is the most often utilized polymer fiber in these THz-regime operations [33Due to its continuous refractive index of 0.1–1.5 THz (Islam et al. 2015b; Hasan et al. 2016b), TOPAS glass also possesses a unique refractory index of 1.53. Because of this, our suggested HX-PCF working frequency range is 0.5–1.5 THz, in order to prevent altering the frequency's influence on TOPAS' refractive index. In addition, TOPAS has a larger coefficient of glass transition temperature, as well as a higher moisture sensitivity (Hasan et al. 2016c). The performance of the suggested hexahedron PCF sensor was evaluated using the finite element approach. This layer absorbs boundary conditions during simulation, as well as a perfectly matched layer (PML). Using FEM, effective Mode Indexes were established to solve Maxwell's balancing. As an anti-reflective surface, the PML limiting layer absorbs PCF waves that are emitted (Islam et al. 2016b). The effective surface area, dispersion loss, V parameters, EML and FPF, and fiber CL are among the numerical characteristics of the THz range. As soon as the COMSOL Multiphysics Version 5 program was launched, the fiber began to spin. The optimum constraints of each cladding diameter $d_1 = 280$ µm, cladding of each pitch $A_c = 385$ µm, core diameter $d_c = 60$ µm, core pitch $A_c = 65$ µm and PML parameters of $P_1 = 2200$ µm and $P_2 = 2450$ µm.

Figure 1(c) indicates the polarization of the optical field distribution at 1 THz of x and y mode. The light confinement is decidedly passed at the core extent that also increases the sensitivity of both x and y polarization of this designed PCF.

3 Discussion and results analysis

We know that the relative sensitivity is determined with the procedure (Islam et al. 2016b):

$$R = \frac{n_a}{n_{eff}} \times P \tag{1}$$

Refractive index for our study was 1.33 for Water. N_{eff} is the effective guided mode index for the analyte, and the value of n_{eff} from the FEM method was obtained in respect of

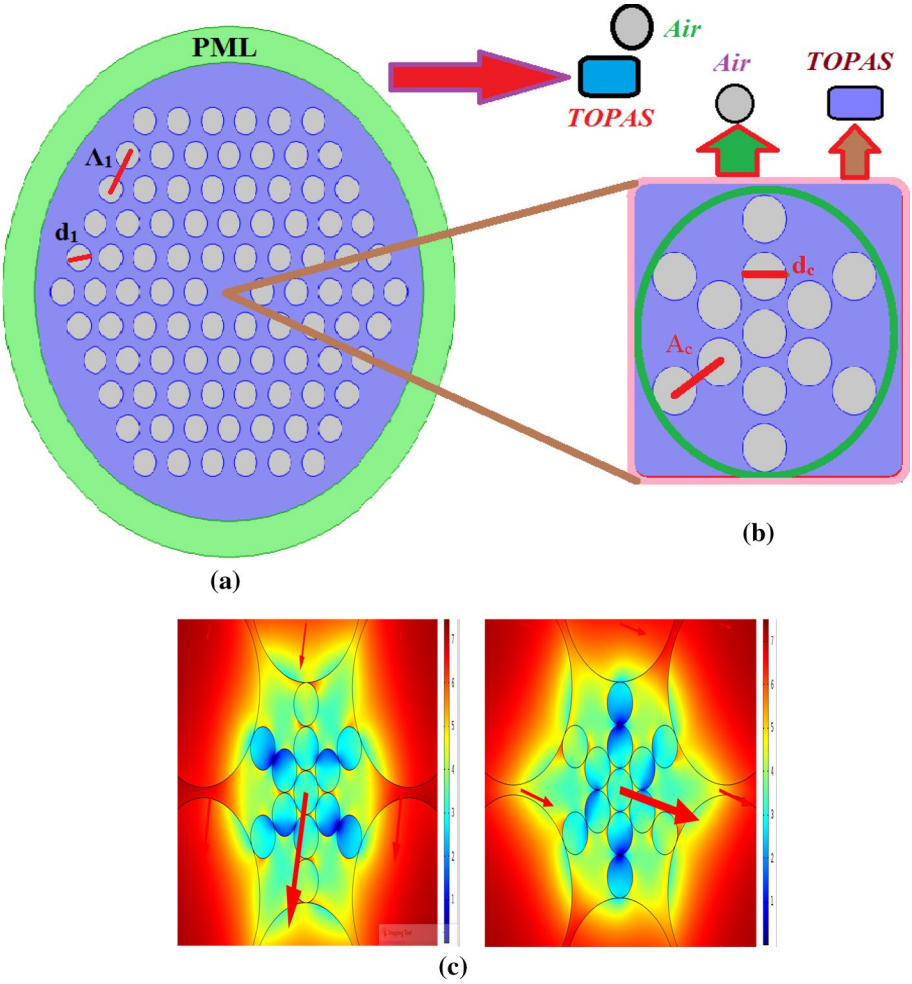

Fig. 1 Pictorial View of **a** Hexagonal cladding, **b** Hexahedron core area, **c** Mode field distributions for both x and polarization

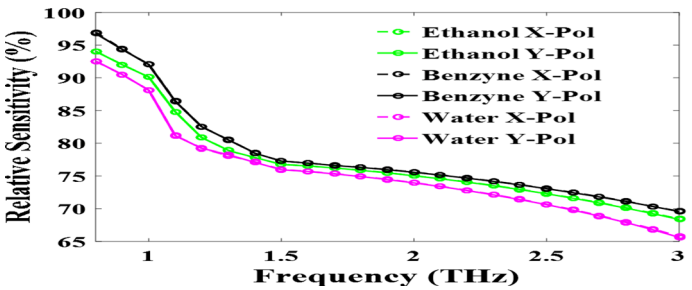

Fig. 2 Sensitivity analysis along with frequency of three chemicals for both at optimum parameters

different frequencies during simulation. Figure 2 shows the efficient mode index value with the frequency for the x- mode and y-mode. The power factor ratio is referred to as P and the mathematical term is (Ahmed et al. 2017):

$$P = \frac{\left[\int \mathrm{Re}(Ex, Hy, Ey, Hx)\mathrm{dxdy}\right]^{1}}{[\int \mathrm{Re}(Ex, Hy, Ey, Hx)\mathrm{dxdy}^{1}} \times 100 \tag{2}$$

where the x-mode and y-mode shows the electric field such as Ex and Ey respectively, Hx and Hy displays the magnetic field of the x and y-direction, respectively.

Figures 2 and 3 for equal divergences with optimal parameters and ± 2% variety parameters are shown in the RS frequency. The RS is similar to added cumulative mode between 1.0 and 0.8 THz from the graphical effect and reduces the RS from 1.10 to 3 THz for Ethanol, Benzene, and Water with frequency diversity. In the case of Ethanol (n = 1.354), Benzene (n = 1.366), and Water (n = 1.330), the relatively sensitive value obtained is 92.65%, 95.25%, and 90.70%.

The RS for benzene, ethanol and water, for the purposes of Fig. 3 are 96.02%, 93.23% and 91.07% for the 1 THz section, the RS for increased (+ 2%) parameters for five layers diameter.

Power fraction (PF) is one of the major properties to check the generation of fiber in various areas. The PF can be evaluated by Hossain et al. (2021d),

$$\eta = \frac{\int_{\mathrm{i}} \mathrm{S_z dA}}{\int_{\mathrm{all}} \mathrm{S_z dA}} \tag{3}$$

In the overall condition, the integration of the number is carried out in interested places such as core, cladding and materials etc. On the other hand, the denominator integration is displayed in the entire intersection area.

Figure 4 stipulates the PF counter with the recurrence at the perfect device. The PF increases from 0.80 to 1.50 THz, and the control division declines from 1.60 to 3 THz after that. After this, the recurrency increases. The highest power fraction standards for three substances: ethanol (n = 1.354), benzene (n = 1.366) and water (n = 1.330) are 74.55, 74.70 and 74.30.

It can be shown in Fig. 5 that the peak rate of PF improves from 0.80 to 1.50 THz and the pinnacle of PF lowers from 1.60 to 3 THz with frequency wave variation. The peak PF standards are 75.40, 76.30, 74.90 for 3 chemicals such as Ethanol (n = 1.354), Benzene (n = 1.366) and Water (n = 1.330). They are 1 THz in increase (+ 2%) parameters for five layers diameter.

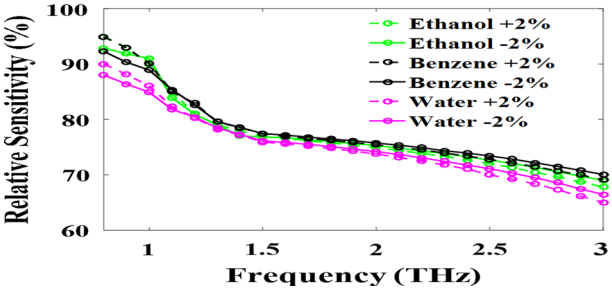

Fig. 3 Sensitivity analysis along with frequency three chemicals for both polarizations at ± 2% variation parameters

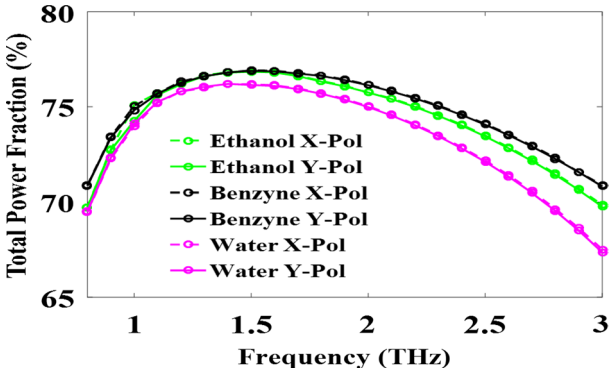

Fig. 4 TPF along with various frequencies for optimal design considerations

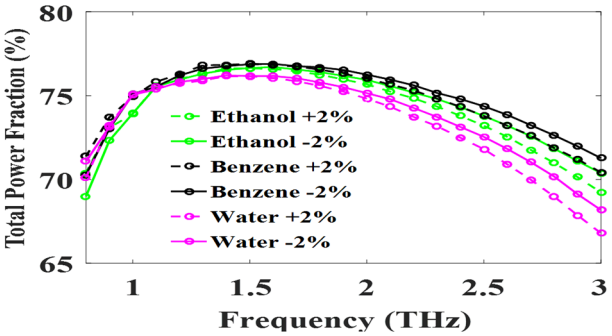

Fig. 5 TPF along with various frequencies at ± 2 Variations

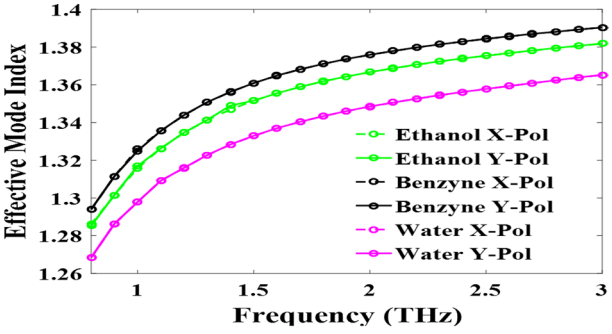

Fig. 6 EMI concerning the frequency of three chemicals for both polarizations at the optimum parameters

The EMI was shown in Fig. 6 for the two divergences of the ideal plan. The efforts to increase the EMI by the recurrence increases are observed. The highest estimate of EMI estimate begins at 1.27 with the recurrence of 0.8 THz, and the highest crest estimate was completed at 1.39, with the largest recurring value at 3 THz. EMI standards for 3 chemicals Ethanol (n = 1354), Benzene (n = 1366), and Water (n = 1330) at 1 THz, 1.29, 1.31 and 1,29 are respectively.

Figure 7 for ± 2% of the varieties with the perfect schedule is shown as opposed to recurrence. The increase in the repeat waves with the EMI was seen to be expanding. In

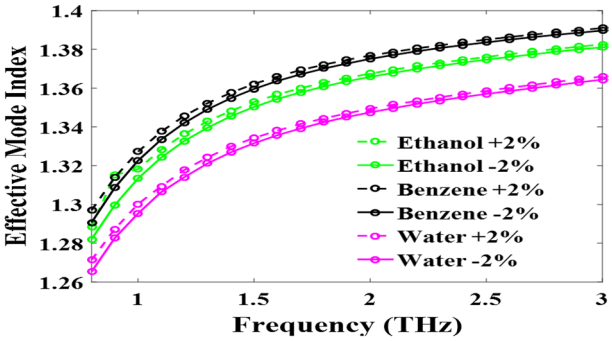

Fig. 7 EMI concerning the frequency of three chemicals for ± 2% variations with the optimum parameters at both polarizations

this case, the EMI's first high esteem is 1.27, with its recurrence extending to 0.8 THz and an exceptional crest appreciation of 1.39, while the recurrence is 3 THz.

Effective area (EA) is the most optical property in any PCF fiber. It is known to us the larger EA-PCF also shows the high RS and the low CL. The effective area (EA) was therefore concluded definitely (Islam et al. 2018a),

$$A_{\text{eff}} = \frac{[\int I(rt)rtdrt]^2}{\left[\int I^2(rt)drt\right]^2}, \quad \text{m}^2 \tag{4}$$

Figure 8 shows the EA that agrees on the recurrence of the hexahedron PCF for superior construction. The EA decreases have concluded here that the recurrence rate increases from 0.8 to 3 THz. Extended effective area (EA) shows the large RS in the THz waveguide. In the process. EA for water, benzene and ethanol in 1 THz operating region 1.39×10^{-7}, 1.65×10^{-7} m^2 and 1.40×10^{-7} m^2.

The fiber is thoroughly designed with TOPAS, a very simple polymer. In any case, polymers are consumed excessively by the higher repetition. Therefore, due to these resources, a few misfortunes are being practiced. The misfortune arising from the tissue is usually known as effective material loss (EML). The effective material loss (EML) is calculated for this exam by following the appointment (Islam et al. 2018a),

$$\text{EML}\left(\alpha_{\text{eff}}\right) = \sqrt{\frac{\varepsilon_0}{\mu_0}}\left(\frac{\int_{\text{mat}} n_{mat|E|^{2\alpha_{\text{mat}}}} dA}{.5 * \left|\int_{all}(E * H \cdot z)dA\right|}\right) (\text{cm}^{-1}) \tag{5}$$

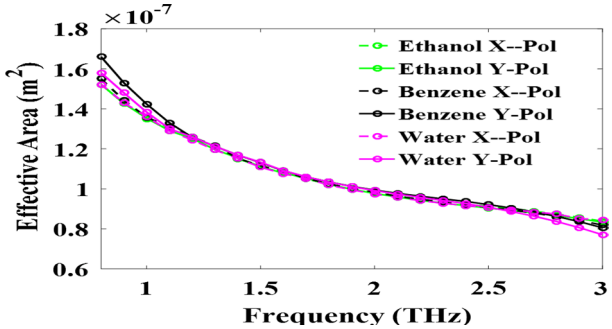

Fig. 8 EA along with various frequencies

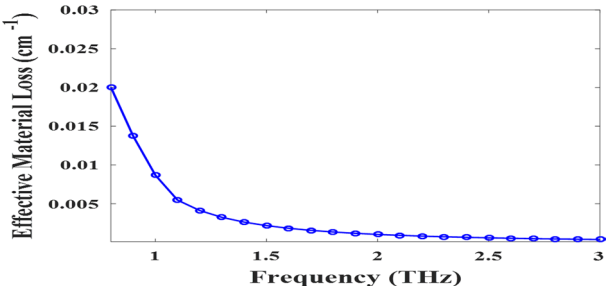

Fig. 9 Effective material loss along with various frequencies for optimum parameters

The H_X-PCF EML was given in Fig. 9 by frequency changes and the EML by increasing frequency. For standard conditions, the EML continue 0.00694 cm^{-1} to 1 THz.

Confinement loss is another visual loss typical of the PCF construction. The low CL-PCF also displays the in-height RS. Here, the expression containment loss was evaluated (Islam et al. 2018a):

$$L_c\left[\frac{dB}{m}\right] = 8.686K_0\ \mathrm{Im}\left[n_{eff}\right], \tag{6}$$

$$K_0 = 2\pi\left(\frac{f}{c}\right), \tag{7}$$

where K_0 is the free wave number and I_m is the imaginary part, f is the frequency and c are the speed of electromagnetic wave ($c = 3 \times 10^8$ ms^{-1}).

Figure 10 shows the reactions of confinement loss (CL) with a recurrence in the optimum plan. The CL decreases to allow the recurrence wave beat to grow. It was also shown that the CLs continue to compete at 2.10–3 THz. The misfortunes of restriction are 5.40×10^{-08}, 6.70×10^{-08} dB/m, and 5.75×10^{-08} dB/m for chemicals like as Ethanol (n = 1.354), Water (n = 1.330) and Benzene (n = 1.366) at 1 THz. We see that the differences of the CL are much smaller than the optimal enterprise strictures of graphic outcomes.

Figure 11 shows that confinement losses (CL) are equal to a recurrence with ideal plan limitations for varieties ± 2%. In accordance with the upgrade of repeatability of the above figure, the CL is decreased. The CL remains consistent as shown in the recurrence from 2.10 to 3 THz. The CL are 7.92×10^{-08}, 7.60×10^{-08} dB/m, and 7.55×10^{-08} dB/m for three chemicals.

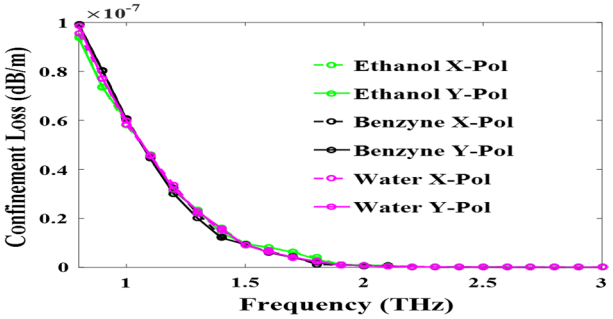

Fig. 10 CL along with different frequencies for optimum design parameters

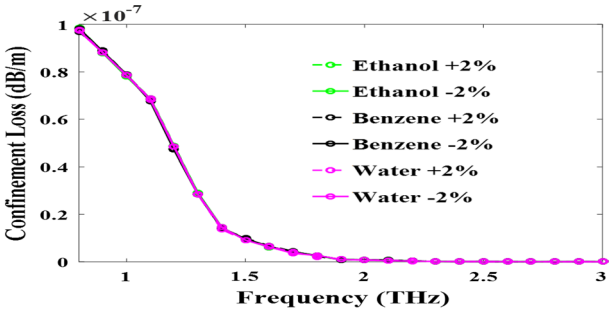

Fig. 11 CL along with different frequencies at ± 2 Variations

V-parameter shows the mode propagation of the PCF structure. So, V-parameter is calculated by the following equation (Islam et al. 2015b):

$$V = \frac{2\pi rf}{c}\sqrt{n_{co}^2 - n_{cl}^2} \leq 2.045 \tag{8}$$

where the core radius is r, n_{co} and n_{cl} are signed by the EMI of the CA and cladding area.

A V-parameter is defined for the working system of the core diameter given in Fig. 12. It shows that the H_X-PCF proposed shows single-mode properties for a long range of diameters. The functional incidence varieties of 0.80–3 THz have been examined in Fig. 12 and the swelling frequency of the V parameter is slightly extended. In addition, the V parameter grade is below 2.405 due to the total functional occurrence range. The proposed H_X-PCF therefore becomes a distinctive methodological complaint that is applicable in the communications system.

The ERI of the PCF directly influences the dispersion profile. The β is the modal propagation constant. It can be acquired from the second order of Taylor expansion that is shown in Islam et al. (2015b):

$$\beta_2 = \frac{2}{c}\frac{dn_{eff}}{d\omega} + \frac{\omega}{c}\frac{d^2 n_{eff}}{d\omega^2}, \quad [\text{ps/THz/cm}] \tag{9}$$

where $N_{eff} = \text{Re}\ (\beta)\omega/c$ and $\omega = 2\pi f$; For propagation mode, there are found two polarizations (x and y polarizations). There are two polarizations in propagation mode (x and y polarizations). The application of Eq was shown in Fig. 13. Figure 13 illustrates well that both polarization curves exert themselves to the left and the right with close-fitting

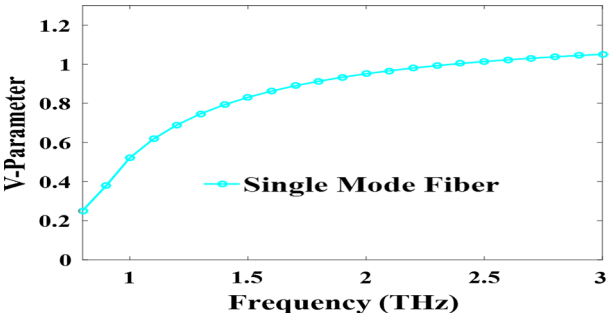

Fig. 12 V-parameter of the designed H_X-PCF is computed at various frequencies for optimum design

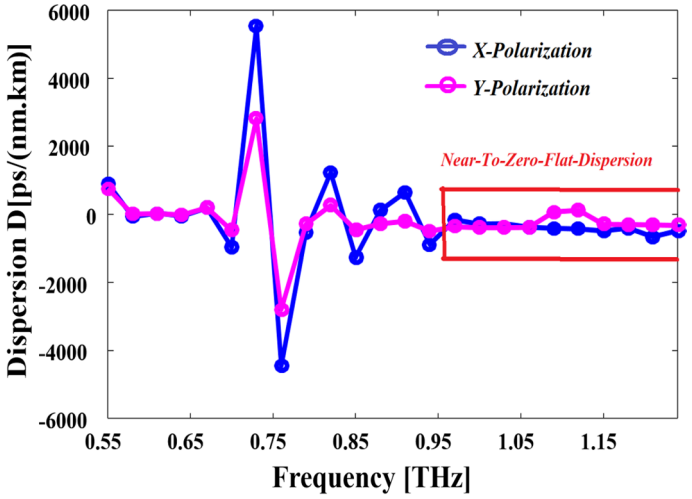

Fig. 13 Dispersion of the designed H_X-PCF is computed at various frequencies for optimum design

behavior. A flat dispersion of 0.97–1.09 THz near zero has been observed in a larger frequency spectrum.

In some cases, multiple optical signals with almost the same pulse spread can be transmitted simultaneously. The lower dispersion value also allows the transmitted optical signal to have a greater bandwidth. There is also a flatted dispersion near zero over a larger frequency spectrum from 0.97 to 1.09 THz. In some cases, multiple optical signals with almost the same pulse spread can be transmitted simultaneously. The lower dispersion value also allows the transmitted optical signal to have a greater bandwidth. This type of behavior with optical parameters gives the proposed fiber a positive degree.

The ideal design and design of optical possibilities such as the RS and the CL of the H_X-PCF have also shown $\pm 2\%$ contrasts. Table 1 clearly shows a small sum of considerable differences between the $\pm 2\%$ variations, and the RS and CL are ideal for relaxation. We thus choose excellent plans to escape the complexity of the manufacture. Therefore, ready to say firmly that for reasons of location for chemicals, the proposed H_X-PCF structure within the industry or biomedicine regions is more

Table 1 The table shows the $\pm 2\%$ variations and the optimum values at the area of 1 THz

Parameters (%)	Relative sensitivity (%)			Confinement loss (dB/m)		
	Water	Ethanol	Benzene	Water	Ethanol	Benzene
+2%	91.07	93.23	96.02	7.55×10^{-08}	7.92×10^{-08}	7.55×10^{-08}
Optimum	90.70	92.65	95.65	5.75×10^{-08}	5.40×10^{-08}	6.70×10^{-08}
−2%	89.40	91.05	94.05	7.45×10^{-08}	7.60×10^{-08}	7.70×10^{-08}

reasonable.

Table 2 The compare table shows optical properties with H_X-PCF structure and others PCFs

Prior in PCFs	Operating region	Relative sensitivity (%)	Confinement loss (dB/m)	Design of structure	
				Core	Cladding
PCF_1 (Hasan et al. 2016c)	f = 1 THz	60.05	1.43×10^{-11}	Rotated-Hexa circular holes	Heptagonal
PCF_1 (Ahmed et al. 2017)	f = 1.2 THz	64.00	1.12×10^{-11}	Elliptical holes	Quasi
PCF_1 (Rana et al. 2014)	f = 1 THz	74.54	7.72×10^{-08}	Slotted core	Quasi
PCF_1 (Saiful Islam et al. 2018a)	f = 1.3 THz	78.80	2.19×10^{-09}	Elliptical holes	Quasi
PCF_1 (Saiful Islam et al. 2018b)	f = 1 THz	45.13	5.583×10^{-05}	Circular holes	Hexagonal
PCF_1 (Hasan et al. 2016b)	f = 1 THz	55.56	1.00	Rhombic holes	Hexagonal
PCF_1 (Hasanuzzaman et al. 2016)	f = 1 THz	80.93	1.23×10^{-11}	Elliptical hole	Circular
Proposed H_X-PCF	f = 1 THz	92.65	5.40×10^{-08}	Hexahedron	Hexagonal

Finally, Table 2 shows that the suggested H_X-PCF is higher than the other PCFs. Thus, in both the optical waveguides and optical devices, the suggested PCF will play a vital role when the PCF is installed.

It is certainly perceived from above study and assessment properties of Table 2 that the proposed PCF design will be play an important role for various chemicals detection in terahertz (THz) technology.

4 Fabrication possibilities

The creative approach is a critical component of the H_X-PCF framework. PCFs are now developed using the most common methods of construction, such as tiresome, sol–gel, passenger plug, stack and attraction. Lately, the Sol–gel (Shuvo et al. 2020; Mou et al. 2019) method has been tested to improve the sensor PCFs. The specific filling approach (Mou et al. 2020b; Islam et al. 2015b), on the other hand, results in the chemicals in the center zones being filled or stacked with any PCF fibers. As a result of selecting the feasible research on this specific supplementary strategy the framework, superior management qualities such as RS, mishaps, EA, TPF, and EMI are raised.

5 Conclusion

We suggested hexagonal cladding and hexahedron core based fiber for sensory and chemical detection. Here, we have used a perfectly matched layer (PML) and finite element method-based COMSOL software to design this fiber (H_X-PCF) and obtain all of the numeric result outputs. 92.65%, 95.25%, and 90.70%, relative Sensitivity and low detainment losses with the value of the body are highest 5.40×10^{-08}, 6.70×10^{-08} dB/m, and 5.75×10^{-08} dB/m. The suggested H_X-PCF sensors were developed at 1 THz for three chemicals, ethanol (n = 1354), benzene (n = 1366), and water (n = 1330), with an effective material loss (EML) of 0.0694 cm^{-1}. The suggested sensor's improved geometrical structure is thought to be production friendly, allowing it to be used in real-world applications such as biomedicine and industry.

Acknowledgements The authors are grateful to the participants who contributed to this research. The authors have not received any funding for this research.

Author contributions All authors are equally contributed of this research work.

Funding The authors have not received any funding for this research.

Availability of data and materials This paper has sufficient data which has been taken from COMSOL Multiphysics software by simulation the work.

Declarations

Conflict of interest The authors declare that they have no competing interests.

References

Abdullah-Al-Shafi, M., Akter, N., Sen, S., Hossain, M.S.: Design and performance analysis of background material of zeonex based high core power fraction and extremely low effective material loss of photonic crystal fiber in the terahertz (THz) wave pulse for many types of communication areas. Optik **243**, 167519 (2021). https://doi.org/10.1016/j.ijleo.2021.167519

Ahmed, K., Chowdhury, S., Paul, B.K., Islam, M.S., Sen, S., Islam, M.I., et al.: Ultrahigh birefringence, ultralow material loss porous core single-mode fiber for terahertz wave guidance. Appl. Opt. **56**(12), 3477–3483 (2017). https://doi.org/10.1364/AO.56.003477

Ahmen, K., Paul, B.K., Chowdhury, S., Sen, S., Islam, M.I., Islam, M.S.: Design of a single mode photonic Crystal fiber with ultra-low material loss and large effective mode area in THz regime. IET Optoelectron. **11**(6), 265–271 (2017)

Chen, L.J., Chen, H.W., Kao, T.F., Lu, J.Y., Sun, C.K.: Low-loss subwavelength plastic fiber for terahertz waveguiding. Opt. Lett. **31**(3), 308–310 (2006)

Gangwar, R.K., Singh, V.K.: Study of highly birefringence dispersion shifted photonic crystal fiber with asymmetrical cladding. Optic **27**(24), 11854–11859 (2016)

Hasan, M.R., Akter, S., Khatun, T., Rifat, A.A., Anower, M.S.: Dual-hole unit-based kagome lattice microstructure fiber for low-loss and highly birefringent terahertz guidance. Opt Eng **56**(4), 043108 (2017)

Hasan, M.M., Barid, M., Hossain, M.S., et al.: Large effective area with high power fraction in the core region and extremely low effective material loss-based photonic crystal fiber (PCF) in the terahertz (THz) wave pulse for different types of communication sectors. J. Opt. (2021). https://doi.org/10.1007/s12596-021-00740-9

Hasan, M.R., Islam, M.A., Anower, M.S., Razzak, S.M.A.: Low-loss and bend-insensitive terahertz fiber using a rhombic-shaped core. Appl. Opt. **55**, 8441–8447 (2016a)

Hasan, M.R., Islam, M.A., Anower, M.S., Razzak, S.M.: Low-loss and bend-insensitive terahertz fiber using a rhombic-shaped core. Appl. Opt. **55**(30), 8441–8447 (2016b). https://doi.org/10.1364/AO.55.008441

Hasan, M.R., Islam, M.A., Rifat, A.A.: A single mode porous-core square lattice photonic crystal fiber for THz wave propagation. J. Eur. Opt. Soc. Rapid. Publ. **12**(1), 15 (2016c). https://doi.org/10.1186/s41476-016-0017-5

Hasanuzzaman, G.K.M., Habib, M.S., Razzak, S.A., Hossain, M.A., Namihira, Y.: Low loss single-mode porous-core kagome photonic crystal fiber for THz wave guidance. J. Lightwave Technol. **33**(19), 4027–4031 (2015)

Hasanuzzaman, G.K.M., Rana, S., Habib, M.S.: A novel low loss, highly birefringent photonic crystal fiber in THz regime. IEEE Photon. Technol. Lett. **28**(8), 899–902 (2016)

Ho, L., Pepper, M., Taday, P.: Terahertz spectroscopy: Signatures and fingerprints. Nat. Photon. **2**(9), 541 (2008)

Hossain, M.S., Barid, M., Sen, S., et al.: Design and analysis of heptagonal cladding with rotated-hexa elliptical core based PCF for the applications of communication sectors in the THz region. Opt Quant Electron **53**, 682 (2021c). https://doi.org/10.1007/s11082-021-03326-8

Hossain, M., Hasan, M., Sen, S., Mollah, M., Azad, M.: Simulation and analysis of ultra-low material loss of single-mode photonic crystal fiber in terahertz (THz) spectrum for communication applications. J Opt Commun (2021). https://doi.org/10.1515/joc-2020-0224

Hossain, M.S., Kamruzzaman, M.M., Sen, S., Azad, M.M., Mollah, M.S.H.: Hexahedron core with sensor based photonic crystal fiber: an approach of design and performance analysis. Sens Bio-Sens Res **32**, 100426 (2021). https://doi.org/10.1016/j.sbsr.2021.100426

Hossain, M.S., Sen, S., Hossain, M.M.: Performance analysis of octagonal photonic crystal fiber (O-PCF) for various communication applications. Phys. Scr. **96**(5), 55506 (2021). https://doi.org/10.1088/1402-4896/abe323

Hossain, M.S., Sikder, A.S., Sen, S., et al.: Design and numerical analysis of Zeonex-based photonic crystal fiber for application in different types of communication networks. J. Comput. Electron. **20**, 1289–1295 (2021d). https://doi.org/10.1007/s10825-021-01704-9

Ilatikhameneh, H., Ameen, T., Chen, F., Sahasrabudhe, H., Klimeck, G., Rahman, R.: Dramatic impact of dimensionality on the electrostatics of P–N junctions and its sensing and switching applications. IEEE Trans. Nanotechnol. (2018). https://doi.org/10.1109/TNANO.2018.2799960

Islam, R., Habib, M.S., Hasanuzzaman, G.K.M., Rana, S., Sadath, M.A., Markos, C.: IEEE Photon. Technol. Lett. **28**, 1537 (2016b)

Islam, R., Rana, S., Ahmad, R., Kaijage, S.F.: Bend-Insensitive and Low-Loss Porous Core Spiral Terahertz Fiber. IEEE Photon. Technol. Lett. **27**(21), 2242–2245 (2015a). https://doi.org/10.1109/LPT.2015.2457941

Islam, R., Rana, S., Ahmad, R., Kaijage, S.F.: Bend-insensitive and low-loss porous core spiral terahertz fiber. IEEE Photon. Technol. Lett. **27**(21), 2242–2245 (2015b). https://doi.org/10.1109/LPT.2015.2457941

Islam, M.S., Rana, S., Islam, M.R., Faisal, M., Rahman, H., Sultana, J.: Porous core photonic crystal fiber for ultra-low material loss in THz regime. IET Commun. **10**(16), 2179–2183 (2016a)

Islam, M.S., Sultana, J., Atai, J., Abbott, D., Rana, S., Islam, M.R.: Ultra low loss hybrid core porous fiber for broadband applications. Appl. Opt. **56**(9), 1232–1237 (2017)

Islam, M.S., Sultana, J., Dorraki, M., Atai, J., Islam, M.R., Dinovitser, A., et al.: Low loss and low dispersion hybrid core photonic crystal fiber for terahertz propagation. Photon. Netw. Commun. **35**(3), 364–373 (2018a)

Lee, Y.S., Lee, C.G., Jung, Y., Oh, M.K., Kim, S.: Highly Birefringent and dispersion compensating photonic crystal fiber based on double line defect core. J. Opt. Soc. Korea **20**(5), 567–574 (2016)

Lee, J.H., Teh, P.C., Yusoff, Z., Ibsen, M., Belardi, W., Monro, T.M., Richardson, D.J.: A holey fiber-based nonlinear thresholding device for optical CDMA receiver performance enhancement. IEEE Photon. Technol. Lett. **14**(6), 876–878 (2002)

Lu, J.Y., Yu, C.P., Chang, H.C., Chen, H.W., Li, Y.T., Pan, C.L., Sun, C.K.: Terahertz air-core microstructure fiber. Appl. Phys. Lett. **92**(6), 064105 (2008)

Mollah, M.S.H., Abdullah-Al-Shafi, M., Hossain, M.S., et al.: An ultra-low material loss ellipse core-based photonic crystal fiber for terahertz wave guiding: design and analysis. J Comput Electron **20**, 1541–1548 (2021). https://doi.org/10.1007/s10825-021-01720-9

Mou, F.A., Rahman, M.M., Islam, M.R., Bhuiyan, M.I.H.: Development of a photonic crystal fiber for THz wave guidance and environmental pollutants detection. Sens. Bio-Sens. Res. **29**, 100346 (2020a). https://doi.org/10.1016/j.sbsr.2020.100346

Mou, F.A., Rahman, M.M., Islam, M.R., Bhuiyan, M.I.H.: Development of a photonic crystal fiber for THz wave guidance and environmental pollutants detection. Sens Bio-Sens Res **29**, 100346 (2020)

Mou, F. A., Rahman, M. M., Mahmud, A. A., Bhuiyan, M. I. H., Islam, M. R.: Design and characterization of a low loss polarization maintaining photonic crystal fiber for THz regime. In: IEEE International Conference on Telecommunications and Photonics (2019)

Rahman, M. M., Mou, F. A., Bhuiyan, M. I. H., Islam, M. R.: Extremely low effective material loss of air core photonic crystal fiber for THz guidance. In: IEEE Region 10 Symposium (TENSYMP), Kolkata, India, pp. 716–720. https://doi.org/10.1109/TENSYMP46218.2019.8971297

Rana, S., Hasanuzzaman, G.K., Habib, S., Kaijage, S.F., Islam, R.: Proposal for a low loss porous core octagonal photonic crystal fiber for T-ray wave guiding. Opt. Eng. **53**(11), 115107–115107 (2014). https://doi.org/10.1117/1.OE.53.11.115107

Rana, S., Rakin, A.S., Hasan, M.R., Reza, M.S., Leonhardt, R.: Low loss and flat dispersion kagome photonic crystal fiber in the terahertz regime. Opt. Commun. **410**, 452–456 (2018a)

Rana, S., Rakin, A.S., Hasan, M.R., Reza, M.S., Leonhardt, R., Abbott, D., Subbaraman, H.: Low loss and flat dispersion Kagome photonic crystal fiber in the terahertz regime. Opt. Commun. **410**, 452–456 (2018b)

Ritari, T., Tuominen, J., Ludvigsen, H., Petersen, J.C., Sorensen, T., Hansen, T.P., Simonsen, H.R.: Gas sensing using air-guiding photonic bandgap fibers. Opt. Express **12**, 4080–4087 (2004)

Saiful Islam, Md., Sultana, J., Ahmed, K., Rakibul Islam, M., Dinovitser, A., Wai-Him Ng, B., Abbott, D.: A novel approach for spectroscopic chemical identification using photonic crystal fiber in the terahertz regime. IEEE Sens. J. **18**, 575–582 (2018a)

Saiful Islam, Md., Sultana, J., Rifat, A.A., Dinovitser, A., Wai-Him Ng, B., Abbott, D.: Terahertz sensing in a hollow core photonic crystal fiber. IEEE Sens. J. **18**, 4073–4080 (2018b)

Shuvo, S., Shafi, M.A., Sikder, A.S., Hossain, Md.S., Azad, M.M.: Zeonex based decagonal photonic crystal fiber (D-PCF) in the terahertz (THz) band for chemical sensing applications. Sens. Bio-Sens. Res. (2020). https://doi.org/10.1016/j.sbsr.2020.100393

Sultana, J., Islam, M.S., Faisal, M., Islam, M.R., Ng, B.W.H., Ebendorf-Heidepriem, H., Abbott, D.: Highly birefringent elliptical core photonic crystal fber for terahertz application. Opt. Commun. **407**, 92–96 (2018)

Vera, E.R., Restrepo, J.U., Durango, C.J., Cardona, J.M., Cardona, N.G.: Design of low loss and highly birefringent porous core photonic crystal fiber and its application to terahertz polarization beam splitter. IEEE Photon. J. **10**(4), 1–13 (2018)

Zhou, J., Zheng, Y.: Fiber refractive index sensor with lateral-offset micro-hole fabricated by femtosecond laser. Optik **185**, 1–7 (2019). https://doi.org/10.1016/j.ijleo.2019.03.094